ChemComm

COMMUNICATION

View Article Online
View Journal | View Issue

Cite this: *Chem. Commun.*, 2024, **60**, 5302

Received 14th February 2024,
Accepted 21st March 2024

DOI: 10.1039/d4cc00735b

rsc.li/chemcomm

Structural effects of oxidation on sugars: glucose as a precursor of gluconolactone and glucuronolactone†

Maider Parra-Santamaria, ‡[ab] Aran Insausti,‡[ab] Elena R. Alonso,§[a] Francisco J. Basterretxea[a] and Emilio J. Cocinero *[ab]

Although structural information on sugars is wide, experimental studies on the oxidation products of sugars in the gas phase, free from solvent interactions, have been rarely reported. We present an experimental work on the changes in the structure and interactions of two products of glucose oxidation (D-glucono-1,5-lactone (GlcL) and D-glucurono-6,3-lactone (GlcurL)) with respect to their precursor. Features such as intramolecular interactions, ring puckering and tautomerism were observed.

Carbohydrates are one of the four pillars of molecular building blocks of biological systems renowned for their key role in physiological processes (*i.e.*, energy suppliers, protein folding and cell signalling and proliferation).[1,2] In addition, their impact in areas of medicinal chemistry in the design of therapeutic agents has also increased notably.[3,4] Structurally, sugars are extraordinarily flexible and even in the most elementary units, such as monosaccharides, the structural typology is huge. Isomeric preferences (pyranose *vs.* furanose or linear chains), conformational choices (*i.e.*, chair and boat configuration in six membered rings or pseudorotation between envelope (E) and twisted (T) configurations in five membered rings), anomeric configurations (α *vs.* β) and the role of the intramolecular interactions (hydrogen bonding) make them able to take on a multitude of forms and functionalities. Literature on the structure of these biomolecules is broad, particularly in the solution and solid state, which has identified a preference for six-membered chair form rings and the axial disposition of the anomeric hydroxyl (OH) group favoured by the anomeric effect.[5,6] More recent gas-phase studies have allowed the analysis of molecules without environmental interference, corroborating the preference for chairs. In addition, all structures are stabilised by cooperative networks of hydrogen bonds (HBs), which in the six-carbon atom sugars adopt a counterclockwise (**cc**) orientation of the hydroxyl groups, while the exocyclic hydroxyl group preferentially adopts a *gauche–gauche* (*gg*) or *gauche–trans* (*gt*) conformation.[7–11]

Oxidation is a half-reaction of utmost relevance in glycobiology, as it allows the synthesis of a wide variety of monosaccharides and their derivatives from simple sugars. It is well known that the three-dimensional shapes of carbohydrates are directly related to the function they will perform in nature. Hence, the structures and therefore the function performed by these oxidation products will be different from those of the original sugar[12] and it is essential to reveal these structural changes. Determining factors for the different conformations of each oxidation product are ring-puckering, hydrogen bonds (HBs) networks, steric effects due to torsional constraints on the ring(s) and anomeric and *gauche* effects. Addressing these factors, we present a pioneering study on two sugar–lactones derived from the oxidation of D-glucose: (**Glc**)-D-gluconolactone (**GlcL**) and D-glucuronolactone (**GlcurL**) (see Fig. 1) – setting the stage for further advancements in the field. **Glc** is the most abundant monosaccharide in nature, which upon oxidation of the OH at its anomeric carbon results in **GlcL** (see pathway a in Fig. 1a) and, on the other hand, **GlcurL** is formed after the oxidation of the hydroxymethyl (CH_2OH) group of **Glc** and then by intramolecular esterification at the C3 carbon (see pathway b in Fig. 1b).

Studies of isolated molecules in the gas phase offer an appealing option as they enable investigations in isolated environments. This approach circumvents potential masking effects introduced by solvents or crystals, allowing for a direct comparison with theoretical data. In this context, rotational spectroscopy offers an unrivalled performance from its inherent high spectral resolution (few kHz), allowing the unambiguous identification of conformers,[13] tautomers,[14] isotopologues[15] and enantiomers.[16] In this work, we have used a strategy that has

[a] *Departamento de Química Física, Facultad de Ciencia y Tecnología, Universidad del País Vasco (UPV/EHU), Campus de Leioa, Ap. 644, Bilbao 48080, Spain*
[b] *Instituto Biofisika (CSIC-UPV/EHU), Bilbao 48080, Spain*

† Electronic supplementary information (ESI) available. See DOI: https://doi.org/10.1039/d4cc00735b.

‡ These authors contributed equally.

§ Current Address: Grupo de Espectroscopía Molecular (GEM), Edificio Quifima, Parque Científico UVa, Universidad de Valladolid, 47005 Valladolid, Spain.

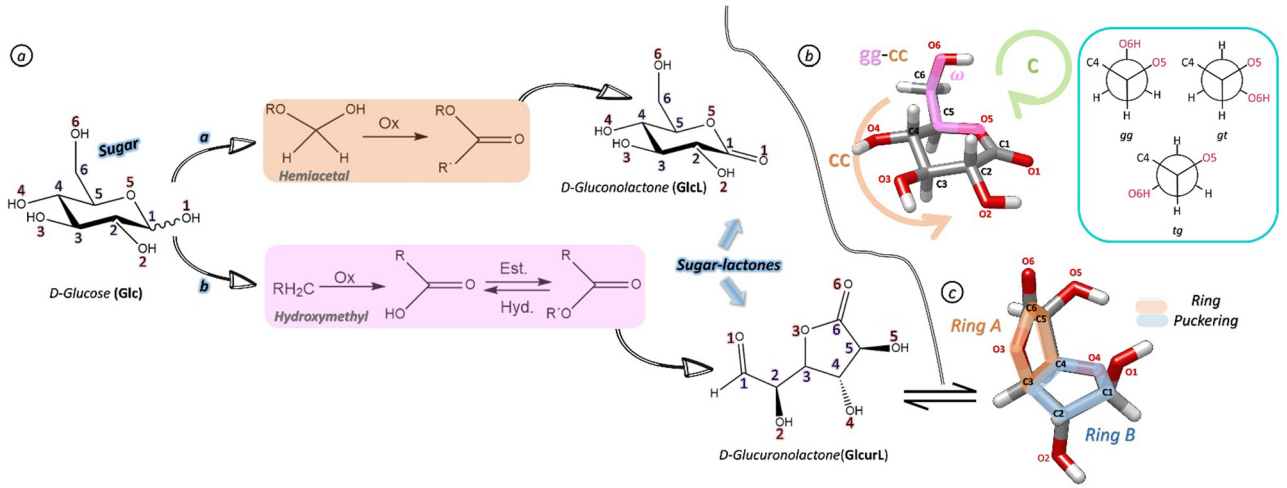

Fig. 1 (a) Scheme of the oxidation reactions from D-glucose (**Glc**) to D-gluconolactone (**GlcL**) (pathway a) and D-glucuronolactone (**GlcurL**, linear form) (pathway b). Reaction intermediates are shown in the orange and pink squares. (b) Labelling used for **GlcL**, together with the three plausible staggered configurations of the CH_2OH group with respect to the sugar ring shown in blue. The green arrow (clockwise, c) and the orange arrow (counter-clockwise, **cc**) show the two possible orientations of the cooperative hydrogen bonding network. (c) Labelling used for **GlcurL** (bicycle furanose form, in chemical equilibrium with the linear one) and ring-puckering marked in orange and blue.

been successful in the case of monosaccharides,[7,10,11] combining rotational spectroscopy coupled with ultrafast laser vaporization into a jet-expansion and computational modelling. Here, the importance of UV ultrafast laser vaporisation deserves to be highlighted, as it made it possible to investigate sugars whose study had been restricted until 2012[7] due to their thermal instability.[17] Building upon these developments and a decade after the first observed sugar by means of microwave spectroscopy, here we report the first rotational analysis of two oxidised monosaccharides whose boiling points make the use of lasers once again indispensable for their measurement.

The project started with an exhaustive conformational search of the potential energy surface (PES) of **GlcL** and **GlcurL** by molecular mechanics (MM) calculations using different force fields to avoid missing any of the possible conformations. Then, the structures corresponding to all identified energy minima were re-optimised by *ab initio* MP2 and density functional theory (DFT) based B3LYP-D3BJ[19,20] methods, implemented in the Gaussian 16 package.[18] In addition, PESs were calculated using the B3LYP-D3BJ level for each system to explore possible interconversions between the conformers of each of the lactones. All calculations were performed using Pople's 6-311++G(d,p) basis set (see ESI† for more detailed information). As for **GlcL**, the key factors in stabilising the plausible conformations for this six-membered ring lactone, which exists in a single anomer due to the lack of an anomeric OH group are: (i) the three staggered orientations of the exocyclic hydroxymethyl group, labelled as described in Fig. 1b, with respect to the cycle frame (*gauche–gauche* (*gg*), *gauche–trans* (*gt*) and *trans–gauche* (*tg*) arrangements); (ii) the orientation of the hydroxyl (OH) groups of the 6-membered ring that associate to establish cooperative networks of intramolecular HBs in a clockwise (**c**) or counterclockwise (**cc**) orientation (Fig. 1b) and (iii) the puckering of the 6-membered ring which can be parameterised by polar coordinates and plotted on a Cremer-Pople (CP) diagram[21] (Fig. S8a, ESI†), where the puckering amplitude q and the phase angles θ and φ span a three-dimensional ring pseudorotation space, which represents the location of an infinite number of conformations of a specific puckering type. Theoretical conformational analysis of **GlcL** showed five structures in an energy window of <7 kJ mol^{-1}. Fig. S1 and S2 (ESI†) display these structures, together with those of the highest predicted energy, while Tables S1 and S2 (ESI†) show the theoretical parameters. The conformers were labelled according to the nomenclature given in Fig. 1b and Fig. S3 (ESI†). According to the CP diagram (see Fig. S11a, ESI†), the four conformers predicted to be the lowest in energy (**GlcL 1–4**) show a similar ring-puckering, adopting an intermediate state between a $^4C_1$-chair and a $^4H_3$-half-chair configuration ($q \approx 0.51$, $\theta \sim 25$–32° and $\varphi \sim 196$–223°). Other configurations in ring puckering such as skew chair ($^1S_3$) are predicted to be higher in energy. All structures are in an energy window <7 kJ mol^{-1} and show a **cc** preference for a cooperative network of intramolecular HBs. However, the theoretical analysis of **GlcurL** was not that straightforward because of the possible existence of five different isomers (Fig. 2) enabled by the absence of oxidation at the anomeric oxygen. Therefore, **GlcurL** (as **Glc**) can exist in linear (l) or cyclic forms in 5- or 6-membered rings (furanose (f) or pyranose (p), respectively), and both α- and β-anomers can be present in the bicyclic forms. Hence, the conformational landscape of the five species had to be interrogated individually. Fig. 2 shows a tentative screening where a preference for **l-GlcurL** and **α-f-GlcurL** forms can be observed. **p-GlcurL** forms were predicted to be very unstable (above >25 kJ mol^{-1}). A representation of the lowest lying energy conformers (Fig. S5–S8, ESI†) for each of the forms, the spectroscopic parameters (Tables S3–S7, ESI†) and the plausible interconversion pathways can be found (Fig. S9) in the ESI.†

Next, the gas-phase rotational spectra of **GlcL** and **GlcurL** were recorded using the Balle–Flygare type cavity Fourier

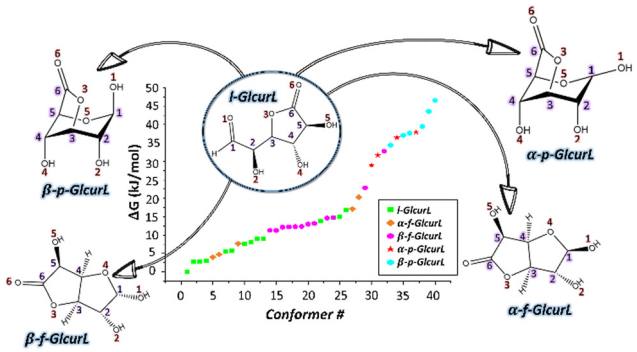

Fig. 2 Structural polymorphism in D-**GlcurL** and predicted Gibbs energies for the 40 most stable conformations calculated using the MP2 method at the 6-311++G(d,p) level of theory.

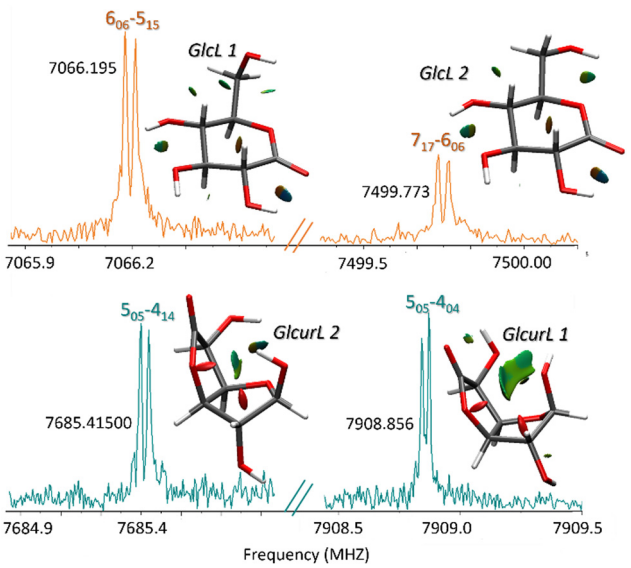

Fig. 3 One experimental rotational transition for each conformer observed in the gas phase of **GlcL** and **GlcurL**. Each transition is doubled by an instrumental Doppler effect. NCI-plots show the existence of HBs in both molecules.

transform microwave (FTMW) spectrometer of the University of the Basque Country (UPV/EHU) coupled to an ultrafast UV-laser vaporisation system described elsewhere[7,22] (see ESI† for further details). The analysis of the rotational spectra allowed us to identify four sets of rotational transitions belonging to independent rotamers. Each transition set was fitted using a semi-rigid rotor Hamiltonian based on Watson's symmetric reduction in the I^r representation[23] to obtain *A*, *B* and *C* rotational constants and quartic distortion constants. Conformational assignments were guided and supported by the computational calculations mentioned above. A direct comparison of the experimental and theoretical rotational parameters (Table 1 and Tables S1–S7, ESI†) allowed us to unambiguously assign the four rotamers to the predicted conformers (Fig. 3). Two of those corresponded to **GlcL** (labelled as **GlcL 1** and **GlcL 2**, based on their predicted energy ranking, according to both B3LYP and MP2 calculations) and two further conformers were observed for **GlcurL**, both in the β-furanose form (**β-f-GlcurL 1** and **β-f-GlcurL 2**). Other isomeric forms of **GlcurL** were exhaustively interrogated but no transitions attributable to these forms were observed. From the structural perspective, **GlcL** adopts a ring-puckered structure intermediate of a $^4C_1$-chair and a half-chair ($^4\mathbf{H}_3$) in the gas phase, this structure is stabilised by a **cc** cooperative network of HBs: O4H → O3H → O2H → O1 and O6H → O5 (Fig. 3, top). The arrangement of the CH_2OH group is the only difference between the two observed conformers, adopting a *gg* orientation for **GlcL 1** and a *gt* disposition for **GlcL 2**. This behaviour is similar to that observed for **Glc**[9] and other monosaccharides where the preference for *gg* and *gt* arrangements and **cc** cooperative networks of HBs are the chosen ones. However, ring distortions of the two conformers of **GlcL** make them have a configuration different to that of **Glc** due to the change in the dihedral angle C5–O5–C1–C2 from −63° in **β-D-Glc** to 25° and 29° in **GlcL 1** and **GlcL 2**, respectively. In the case of **GlcurL**, the experimentally observed conformers are in the β-furanose form, with both the ring puckering ($^2E/^4T_5$ *vs.* $^4T_3/^4T_3$) (see Fig. S8b, ESI†) and the hydrogen bonds stabilising them very differently (see Fig. 3, bottom). In both lactones, the heavy atom disposition of the most stable structures observed in the gas phase was in good agreement with the one observed in the crystal.[24,25] Energetically, the case of **GlcL** is again simpler and correlates very well with the two most stable conformers predicted computationally (Tables S1 and S2, ESI†). The **GlcurL** system needs to be analysed more carefully due to structural polyforms with five plausible tautomers. Fig. 2 illustrates that **l-GlcurL** or **α-f-GlcurL** are expected to be highly predominant in the gas phase. However, as stated above, only two conformers of the β-furanose form were experimentally observed (12 kJ mol^{-1} over linear form), although

Table 1 The main experimental parameters and the predicted data at the MP2/6-311++G(d,p) level for **GlcL** and **GlcurL**. The vibrational contribution in the rotational constants was done using anharmonic calculations at the B3LYP-D3BJ/6-311++G(d,p) level of theory (all details in the ESI). See Table S18, ESI with all experimental spectroscopic parameters

	GlcL 1		**GlcL 2**		**β-f-GlcurL 1**		**β-f-GlcurL 2**	
	Exp.	Theor.	Exp.	Theor.	Exp.	Theor.	Exp.	Theor.
A_0/MHz	1202.45777 (25)[a]	1198	1232.31932 (30)	1221	1656.56600 (17)	1649	1578.36796 (26)	1569
B_0/MHz	844.55185 (21)	837	798.73238 (19)	795	874.851218 (84)	873	806.99379 (12)	802
C_0/MHz	552.81321 (10)	547	502.244063 (77)	499	782.182652 (82)	781	777.96259 (15)	768
N^b	51	—	34	—	104	—	59	—
σ^c/kHz	2.5	—	1.4	—	2.2	—	4.6	—
ΔE_0/kJ mol^{-1}	—	0.0	—	2.6	—	0.0	—	0.7

[a] Standard error in parentheses in the units of the last digits. [b] Number of distinct frequencies in fit. [c] Root mean square error of the fit.

they are predicted to be the most stable within this family. This leads us to suggest that our commercial sample contains only the observed **β-f-GlcurL** form, and the mutarotation is inhibited in the gas phase, which would explain the absence of the other structural isomers, as it could be expected based on previous studies on sugars.[10]

Relative populations of the observed conformers of **GlcL** could also be estimated experimentally by microwave spectroscopy through relative intensities of the observed rotational transitions (see relative populations in the ESI†). Thus, the experimental population ratio is **84 : 16(2)** for **GlcL 1 : GlcL 2** in Ar, which is equivalent to the corresponding to an energy difference of 4.5 kJ mol^{-1} assuming a Boltzmann distribution at 298 K. The latter agrees well with the theoretical value obtained by both the MP2 and B3LYP-D3BJ methods. The experimental relative populations for **β-f-GlcurL** were not determined since the intensities of the rotational transitions of the molecule were not directly comparable. Additionally, in order to confirm the presence of the cooperative hydrogen-bonding network in the assigned conformers and other possible non-covalent interactions (NCIs), topological analyses of the reduced electronic density with the non-covalent interaction (NCI) plots method were carried out. Both NCI plots for **Glc** and **GlcL** (see Fig. S7, ESI†) present a similar panorama that confirms the existence of strong stabilising interactions corresponding to the cooperative network *via* intramolecular HBs previously described (O4H → O3H → O2H → O1 and O6H → O5). However, the structural change after the oxidation of **Glc** to **GlcL** produces a change in the ring-puckering which induces a variation in bond distances near the carbonyl group formed. Specifically, C5–C1 and C1–O1 are considerably shorter in **GlcL** (1.35 Å and 1.21 Å, respectively) than in **β-D-Glc** (1.42 Å and 1.39 Å) as it could be expected. The same trend is observed for the hydrogen bond formed between O1 (in the carbonyl group) and O2H where **β-D-Glc** establishes a 2.47 Å HB and **GlcL** a 2.19 Å one. As for **β-f-Glcur 1**, NCI plots confirm the presence of three non-cooperative weak intramolecular HBs (O1H → $O4_{hemiacetal}$, O2H → $O4_{hemiacetal}$ and O5H → $O6_{carbonyl}$), whereas **β-f-GlcurL 2** presents just two but stronger HBs (O1H → $O3_{ester}$ and O5H → $O4_{hemiacetal}$) according to Fig. 3. According to the NCI analysis for this lactone, we can state that the change in the structure adopted after the generation of two rings in **GlcurL** does not give rise to a cooperative network of OH···OH interactions. In fact, strong destabilising interactions are observed (red cigar-shaped surface), which could be due to the strain caused by the ring structure.

The results of this work mark a milestone, as oxidised glucose products have been effectively transferred to the gas phase *via* ultrafast laser vaporization, allowing the first rotational analysis of this kind of compound. Moreover, it has been proven that the use of rotational spectroscopy (supported by computational calculations) in combination with ultrafast laser vaporisation systems, is not only a very suitable technique for the analysis of intramolecular interactions and structural determination of sugars but also for sugar derivatives, such as sugar–lactones. These results underscore the importance of structural studies based on the combination of rotational spectroscopy and quantum chemistry methods in the gas phase and the need for further experiment-guided theoretical developments: although the studied systems were structurally simple, an exhaustive conformational search was essential to avoid missing any conformations. Benefitting from the continuous advances in the combination of the chirp-excitation technique and laser ablation systems, this work could serve as a basis for future studies on the structural changes and intra/intermolecular interactions after solvation of these molecules, which is crucial for understanding how these changes would affect their biological properties.

We thank the Spanish Government-MCIN, PID2020-117892RB-I00 for financial support, the Basque Government (IT1162-19, PIBA 2018/11, and predoctoral and postdoctoral fellowships to A. I.) and the UPV/EHU (PPG17/10, GIU18/207 and predoctoral fellowship to M. P.-S.). E. R. A. thanks Ministerio de Ciencia e Innovación for a Juan de la Cierva de formación grant (FJC2018-037320-I). Laser and NMR resources of the UPV/EHU together with computational resources of CESGA (Centro de Supercomputación de Galicia) and UPV/EHU (SGIker and I2Basque) were used in this work.

Conflicts of interest

There are no conflicts to declare.

References

1 B. O. Fraser-Reid, *et al.*, *Glycoscience: Chemistry and Chemical Biology*, Springer, Berlin, 2nd edn, 2009.
2 A. Varki, *et al.*, *Essentials of Glycobiology*, Cold Spring Harbor Laboratory Press, New York, 2nd edn, 2009.
3 D. Solís, *et al.*, *A guide into glycosciences: How chemistry, biochemistry and biology cooperate to crack the sugar code*, Elsevier B.V., 2015, 1850.
4 H. J. Gabius, S. André, J. Jiménez-Barbero, A. Romero and D. Solís, *Trends Biochem. Sci.*, 2011, **36**, 298–313.
5 A. L. Lehninger, *Principles of Biochemistry*,ed W. H. Freeman, 4th edn, 2004.
6 M. L. Sinnott, *Carbohydrate Chemistry and Biochemistry: Structure and Mechanism*, The Royal Society of Chemistry, 2007.
7 E. J. Cocinero, *et al.*, *Angew. Chem., Int. Ed.*, 2012, **51**, 3119–3124.
8 E. J. Cocinero, *et al.*, *J. Am. Chem. Soc.*, 2013, **135**, 2845–2852.
9 J. L. Alonso, *et al.*, *Chem. Sci.*, 2014, **5**, 515–522.
10 C. Calabrese, *et al.*, *J. Phys. Chem. Lett.*, 2019, **10**, 3339–3345.
11 I. Peña, *et al.*, *Angew. Chem., Int. Ed.*, 2013, **52**, 11840–11845.
12 G. Hua and K. Odelius, *ACS Sustainable Chem. Eng.*, 2016, **4**, 4831–4841.
13 I. Uriarte, S. Melandri, A. Maris, C. Calabrese and E. J. Cocinero, *J. Phys. Chem. Lett.*, 2018, **9**, 1497–1502.
14 J. L. Alonso, V. Vaquero, I. Peña, J. C. Lõpez, S. Mata and W. Caminati, *Angew. Chem., Int. Ed.*, 2013, **52**, 2331–2334.
15 D. Banser, M. Schnell, J. U. Grabow, E. J. Cocinero, A. Lesarri and J. L. Alonso, *Angew. Chem., Int. Ed.*, 2005, **44**, 6311–6315.
16 D. Patterson, M. Schnell and J. M. Doyle, *Nature*, 2013, **497**, 475–477.
17 R. A. Motiyenko, E. A. Alekseev, S. F. Dyubko and F. J. Lovas, *J. Mol. Spectrosc.*, 2006, **240**, 93–101.
18 M. J. Frisch, *et al.*, *Gaussian 16, Rev. C. 01*.
19 C. Lee, W. Yang and R. G. Parr, *Phys. Rev. B*, 1988, **37**, 785–789.
20 A. D. Becke, *J. Chem. Phys.*, 1993, **98**, 5648–5652.
21 D. Cremer and J. A. Pople, *J. Am. Chem. Soc.*, 1975, **97**, 1354–1358.
22 E. J. Cocinero, A. Lesarri, P. Écija, J. U. Grabow, J. A. Fernández and F. Castaño, *Phys. Chem. Chem. Phys.*, 2010, **12**, 12486–12493.
23 J. K. G. Watson, *Vibrational Spectra and Structure*, New York, Amsterdam, 1977.
24 M. L. Hackert and R. A. Jacobson, *J. Chem. Soc. D*, 1969, 1179.
25 S. H. Kim, G. A. Jeffrey, R. D. Rosenstein and P. W. R. Corfield, *Acta Crystallogr.*, 1967, **22**, 733–743.